Journal of the American College of Cardiology
© 1999 by the American College of Cardiology
Published by Elsevier Science Inc.

Vol. 35, No. 1, 2000
ISSN 0735-1097/00/$20.00
PII S0735-1097(99)00486-6

Acute and Chronic Tissue Response to Coronary Stent Implantation: Pathologic Findings in Human Specimen

Peter H. Grewe, MD,* Thomas Deneke, MD,* Abderrahman Machraoui, MD,* Jürgen Barmeyer, MD, Klaus-Michael Müller, MD†

Bochum, Germany

OBJECTIVES The aim of our study was to analyze the cellular components of neointimal tissue regeneration after coronary stenting.

BACKGROUND High restenosis rates are a major limiting factor of coronary stenting. To reduce the occurrence of restenoses, more insights into the mechanisms leading to proliferation and expression of extracellular matrix are necessary.

METHODS Twenty-one autopsy cases with coronary stents implanted 25 h to 340 days before death were studied. The stented vessel segments were analyzed postmortem by light microscopy and immunohistochemical staining.

RESULTS In the initial phase stents are covered by a thin multilayered thrombus. Alpha-actin–positive smooth muscle cells (SMCs) are found as the main cellular component of the neointimal tissue. Later (>6 weeks) extracellular matrix increases and fewer SMCs can be found. In every phase the SMC layers are loosely infiltrated by inflammatory cells (T lymphocytes). In the early postinterventional phase all endothelial cells are destroyed. The borderline between the vessel lumen and the vascular wall is constituted by a thin, membranous thrombus. Six weeks after stenting, SMCs form the vessel surface. Complete reendothelialization is first found 12 weeks after stenting.

CONCLUSIONS Stent integration is a multifactorally triggered process with proliferating SMCs generating regenerative tissue. In the early phase predominantly thrombotic material can be observed at the site of stenting, followed by the invasion of SMCs, T lymphocytes and macrophages. The incidence of delayed reendothelializations and the occurrence of deep dissections may be associated with excessive SMC hyperplasia. (J Am Coll Cardiol 2000;35:157–63) © 1999 by the American College of Cardiology

Progressive optimization of implantation techniques involving minimally invasive endoprosthesis therapies (stenting) and modification of the medical regimen have helped to reduce early complication rates after coronary stenting (1). Higher expansion pressures and improved medical regimens like the use of ticlopidine, aspirin, clopidogrel and glycoprotein IIb/IIIa receptor inhibitors resulted in a reduction of early complication rates after coronary stenting (2–4). In contrast, the occurrence of in-stent restenosis still remains an unsolved issue. Aside from a rather high incidence of in-stent restenosis within the first months after stenting, one of the major limitations is related to the treatment options (5). After coronary stenting, restenosis rates from 20% to 50% are found. A significant reduction of lumen cross-sectional area is found more often in long coronary stenoses. Highest restenosis rates have to be expected after multiple, overlapping stent insertion or after stenting of small coronary vessels with diameters <3 mm (6,7).

Analysis of the mechanism of stent integration by intravascular ultrasound (IVUS) has demonstrated that stent compression does not contribute to restenosis (8,9). So far there is no evidence for a proliferating and regenerating process of all parts of the vessel wall (remodeling) as a major component of restenosis (10). Animal studies using IVUS and histomorphologic analysis of neointimal material excised from humans have shown that a focally accentuated intimal tissue response occurs after stent implantation. This tissue response is caused by migration and excessive proliferation of smooth muscle cells (SMCs) (11–14). Because tissue identification and characterization is not possible using IVUS, animal studies were designed to define the histologic tissue response (neointima) after stenting (13,15). The application of data from currently available animal models to the human restenosis mechanism after stent

From the *Department of Cardiology and Angiology and †Institute of Pathology, University Hospital "Bergmannsheil," Bochum, Germany.

Manuscript received August 26, 1998; revised manuscript received July 29, 1999, accepted September 14, 1999.

Abbreviations and Acronyms
CD = cluster of differentiation
IVUS = intravascular ultrasound
L-316 = chromium-nickel-ferrum stainless steel
SMC = smooth muscle cell

implantation is limited by species-specific tissue reactions. Considering these species-specific differences and the implantation into undiseased artery segments, animal studies might differ considerably from studies of human arteriosclerotic arteries.

The aim of our study was to characterize the histologic and immunohistochemical cellular and matrix interactions between human vascular walls and coronary stents.

METHODS

The tissue response to 31 stainless-steel coronary stents of 21 patients 25 h to 340 days after implantation was analyzed postmortem. The stented segments were identified by coronary angiography of the isolated hearts after death. Postmortem analysis was performed in the first 24 h after death. After 72-h, 5% formalin pressure fixation of the dissected coronary artery, the stented segment was cut into halves. The two parts of the stent were prepared in different ways. The first half was plastic-embedded into methylmethacrylate (Technovit 9100, Kulzer, Germany), and cross sections were produced using the hardcut-grinding technique (Accutom 5000, Wirtz-Bühler, Germany). By applying this method of preparation using a rotating hardcut microtome, serial cross sections (interspace 0.3 mm) were obtained. Automated precision polishing (Phönix, Wirtz-Bühler, Germany) to a thickness of 10 μm per cross section was performed (complete details of the methods will be provided by the authors upon request). Artifact-free samples are available for staining (modified Ladewig staining) and microscopic analysis. Quantitative analysis was performed using our computer-based video morphometry unit (VIDAS-Video, Zeiss, Germany). After excision of the metal struts, the second half of the stent region was processed for immunohistochemical staining. Immunohistochemical staining with alpha$_1$ actin, factor VIII, cluster of differentiation (CD)3, CD21 and CD68 was performed under standard conditions. Immunohistochemical characterization of the inflammatory cells was possible only in stents already incorporated by neointima (n = 12). Table 1 shows the patient characteristics of the analyzed cases.

RESULTS

Histopathologic Study and Light Microscopy

Light microscopy and video-based morphometry of the stented cross sections revealed inhomogeneous stent expansion in eccentric and concentric arteriosclerotic stenoses. The stents were underexpanded over calcified arteriosclerotic segments of the vessel wall and, in these parts, did not contribute to the initial lumen gain. In parts of the vascular segments with elastic fibrous arteriosclerotic disease, over-

Table 1. Patient Characteristics After Postmortem Analysis

Subject No.	Gender	Age (yrs)	Time After Treatment	Cause of Death	Factor VIII Staining	Actin Staining	Treated Vessel	Stent Type
10/95	F	70	95 d	Ex. card.	+	+	LAD	Palmaz-Schatz
30/95	M	56	32 h	Cardiac	−	−	LAD	Palmaz-Schatz (3 stents)
38/95	M	71	61 d	Ex. card.	−	+	LAD	Palmaz-Schatz
122/95	M	67	28 d	Ex. card.	−	+	LAD	DEVON
243/95	M	54	12 d	Cardiac	−	−	LAD	MICRO (2 stents)
382/95	M	64	10 d	Cardiac	−	−	LAD	MICRO
291/96	M	70	96 d	Ex. card.	+	+	Bypass	DEVON (2 stents)
291/96	M	70	124 d	Ex. card.	+	+	Bypass	DEVON
365/96	M	76	11 d	Ex. card.	−	−	LAD	Multi-Link
31/97	F	81	9 d	Cardiac	−	−	RCA	NIR Cordis (3 stents)
53/97	F	73	150 d	Cardiac	+	+	LCx	Palmaz-Schatz
103/97	F	65	311 d	Cardiac	+	+	LAD	NIR Cordis
123/97	M	74	40 d	Cardiac	−	+	RCA	DEVON
174/97	M	78	90 d	Ex. card.	+	+	LAD	MICRO
324/97	M	71	30 d	Cardiac	−	+	LAD	NIR
324/97	M	71	101 d	Cardiac	+	+	LCx	Roubin
929/98	M	38	340 d	Cardiac	+	+	LAD	Palmaz-Schatz
68/98	M	65	25 h	Cardiac	−	−	RCA	NIR Cordis (2 stents)
154/98	M	68	48 h	Cardiac	−	−	RCA	DEVON
223/98	F	76	229 d	Cardiac	+	+	RCA	Roubin (2 stents)
223/98	F	76	118 d	Cardiac	+	+	LAD	Palmaz-Schatz (3 stents)

Ex. card. = extracardiac; F = female; LAD = left anterior descending coronary artery; LCx = left circumflex coronary artery; M = male; RCA = right coronary artery.

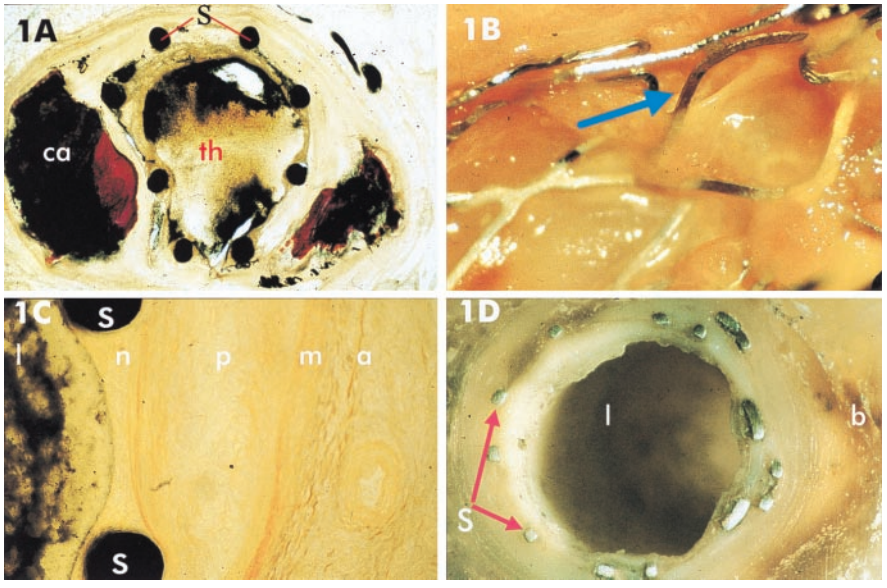

Figure 1. **A,** Light microscopic specimen (subject no. 243/95). Histologic cross section of a stented coronary artery. Implantation pressures of 15 atm did not produce complete stent expansion. Subacute stent thrombosis after 12 days. Lumen obstructed by thrombotic material (th). Extensive calcification (ca) impeding complete homogeneous stent expansion. S = stent strut. (Magnification ×11, reduced by 65%.) **B,** Gross specimen (subject no. 365/96). Longitudinally dissected coronary artery 11 days after stenting. The endoprosthesis is incompletely covered by a thin, membranous thrombus →. In between stent filaments multiple intramural hematomas can be identified. (Magnification ×7.) **C,** Light microscopic specimen (subject no. 122/95) of a histologic cross section of a coronary artery 28 days after stenting. Stent struts (S) show coating by neointima (n) with few cellular infiltrates. The borderline between neointima and arteriosclerotic plaque (p) is still visible. Lumen (l) filled with contrast medium after postmortem coronary angiography. m = media; a = adventitia. (Magnification ×25, reduced by 65%.) **D,** Gross specimen (subject no. 291/96). Longitudinal section of a coronary artery six months after stent implantation. Stent struts (S) covered by gray neointima. Intercellular hemosiderin pigments as residuals of intramural bleedings (b) caused by the implantation trauma in the outer media. l = lumen. (Magnification ×8.5, reduced by 65%.)

expansion of the endoprosthesis could be seen leading to deep impression of the stent filaments into the soft plaques. A gain in stent symmetry by high pressure stenting was not found (Fig. 1A).

With intraindividual differences, the generation of the stent neointima can be divided into two different time phases (Table 2). The regeneration of the endothelial border seems to occur in three different time phases (Table 3).

Table 2. Phases I and II of Neointimal Generation

I.	Phase of Reparation
	Intramural hematoma after intimal plaque rupture or dissection of the media
	Generation of a membranous mural thrombus (including red blood cells, neutrophils, aggregations of thrombocytes)
	Loosely structured matrix components
II.	Phase of Proliferation
	Initial increase of SMCs
	Progressive solidification of matrix structure
	Loose infiltration by lymphocytes
	Lymphocytic aggregation around stent struts
	Matrix cover around stent struts without SMCs

SMCs = smooth muscle cells.

Phase I of Neointimal Generation: Reparation

Eleven to 16 days after stenting only incomplete tissue coverage of the endoprosthesis (Fig. 1B) was documented. Complete coating of the stents was first found 28 days after stent implantation. This early neointima contains almost no matrix structures. It consists of a basis of thrombotic material with incorporated red blood cells, aggregated thrombocytes and neutrophil granulocytes. Four weeks after stenting a focal augmentation of extracellular matrix is observed in those parts of the vascular wall compressed by stent struts. In this early phase, lymphocytes as a major part of an inflammatory response are accentuated in neointimal segments directly adjacent to the stent struts, but they can

Table 3. Phases I–III of Endothelial Regeneration

I.	Phase: Endothelial Denudation
	Destruction of the endothelial vessel wall lining in the implantation zone
II.	Phase: Reendothelialization
	Neointimal surface covered by matrix and SMCs
	Spots of neoendothelium
III.	Phase: Neoendothelium
	Complete coverage by factor VIII–positive cells of endothelial origin

SMCs = smooth muscle cells.

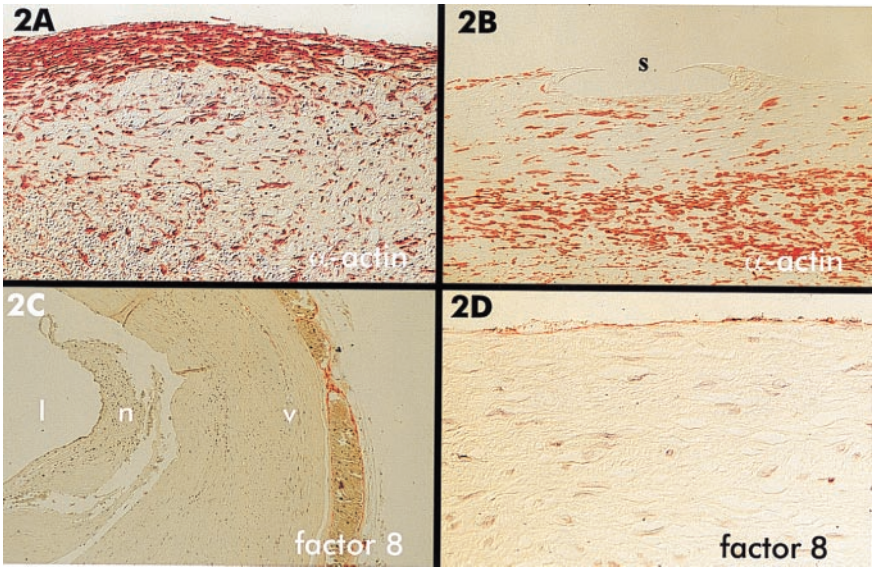

Figure 2. A, Immunohistochemical staining (alpha-actin). Neointima 101 days after stenting (subject no. 324/97). Compact layer of alpha-actin testing positive cells (red) in the luminal zone of the intima. Loose infiltration with alpha-actin–positive cells of the intercellular matrix in the thicker, outer layer of the neointima. (Magnification ×45, reduced by 65%.) **B,** Light microscopic specimen. Stent neointima after removal of the stent struts (s) (subject no. 174/97). Directly adjacent to the alloplastic stent filaments no alpha-actin–positive SMCs (red) can be detected. (Magnification ×45, reduced by 65%.) **C,** Immunohistochemical staining after removal of stent struts (subject no. 38/95). Factor 8-negative cells form the borderline between the lumen (l) and neointima (n) 68 days after stenting. Endothelial cells of the hyperemic vasa vasorum (v) are tested factor 8–positive. Indentation of stent struts. (Magnification ×35, reduced by 65%.) **D,** Immunohistochemical staining (factor 8-positive = red). Complete endothelialization of the neointima by mature endothelial cells 101 days after stenting (subject no. 324/97). **Upper,** lumen; **lower,** neointima (distal stent). (Magnification ×75, reduced by 65%.)

be found uniformly distributed over the complete stented artery segment.

In between stent struts, the neointimal tissue measures up to 120 μm from the arterial media to the lumen. At points over the stent filaments the neointima measures only a few micrometers (Fig. 1C).

Phase II of Neointimal Generation: Proliferation

Over the time course of incorporation, a decrease in inflammatory infiltration and an increase of SMC and extracellular matrix was documented. Higher numbers of SMCs went along with increasing neointimal volume. The effects of the implantation trauma were still visible nine months after stenting—large, only partially organized intramural hematomas (Fig. 1D). The thickness of the neointima was found to be between 110 μm 40 days after and 450 μm 321 days after stent incorporation.

Immunohistochemical Analysis

Neointima. Twenty-eight days after stent implantation some alpha-actin–positive cells (SMCs) start to migrate into the arterial wall. These cells are embedded into a loose extracellular matrix with only a few fiber bundles. An increase of more concentric, circular-aligned tissue is found over the time course after stenting. By testing alpha-actin, a focally accentuated accumulation of SMCs was seen in the neointima in all cases (Fig. 2A).

More than 12 weeks after stenting, the neointima consists of a three-layered tissue with intra-individual differences:

1) Alpha-actin–positive cells are located in the luminal area of the neointima. The alpha-actin–positive SMCs are circular-aligned and interposed onion-like. This layer consists of 15 to 30 cell layers.
2) The adjacent, middle layer appears less cellular. Only a few SMCs are embedded into a thick layer of intercellular matrix. There is almost no cellular interdigitation in between the alpha-actin–positive cells.
3) The outer part of the neointima becomes more cellular >3 months after stenting, building a thick cellular stratum. This layer continuously extends into the original medial lamina of the vascular wall or into the SMC cover found in plaque caps of arteriosclerotic lesions.

The tissue response after stenting usually produced concentric narrowing of the lumen. A focally accentuated increase in neointimal thickness was based on intramural bleeding. These hematomas are found to be in different phases of organization.

Arteriosclerotic plaques proximal and distal to the stented segments show different vessel wall structures than the stent neointima. Smooth muscle cells are accumulated in the surface near plaque cap. The central lipid-rich plaque zone is dominated by cholesterol crystals and CD68-positive macrophages with only a few alpha-actin–positive cells (SMCs).

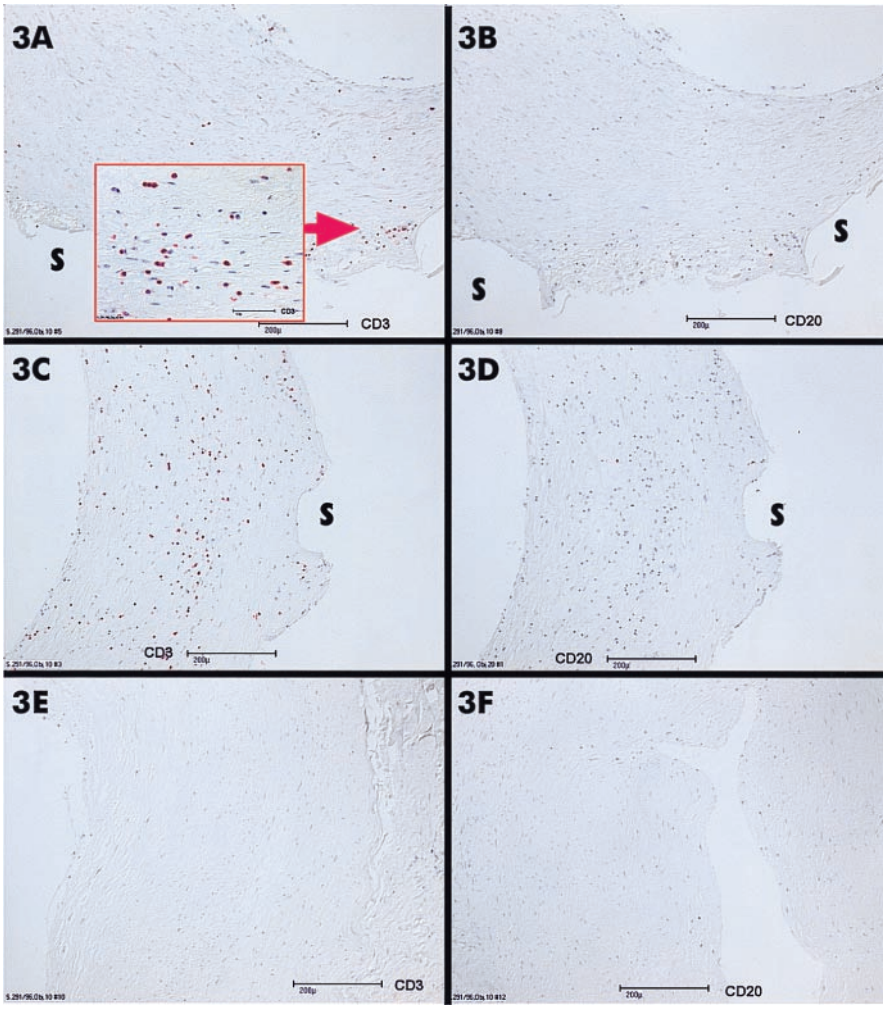

Figure 3. **A,** Immunohistochemical staining (CD3-positive = red). Neointima 96 days after stenting (subject no. 291/96). CD3-positive T lymphocytes aggregated around the stent struts. Impression of a removed stent filament in the lower right of the figure. Magnification: CD3-positive cells. s = stent strut. (Magnification ×35, reduced by 65%.) **B,** Immunohistochemical staining (CD20-positive = red). Neointima 96 days after stenting (subject no. 291/96). No CD20-positive B lymphocytes in the stent neointima. s = stent strut. (Magnification ×35, reduced by 65%.) **C,** Immunohistochemical staining (CD3-positive = red). Neointima 124 days after stenting. Diffuse infiltration by CD3-positive T lymphocytes in this phase of stent integration. s = stent strut. (Magnification ×35, reduced by 65%.) **D,** Immunohistochemical staining (CD20-positive = red). Neointima 124 days after stenting (subject no. 291/96). No CD20-positive B lymphocytes in the stent neointima. s = stent strut. (Magnification ×35, reduced by 65%.) **E,** Immunohistochemical staining (CD3-positive = red). No CD3-positive T lymphocytes in the vessel segment 2 cm proximal to the stent (subject no. 291/96). (Magnification ×45, reduced by 65%.) **F,** Immunohistochemical staining (CD20-positive = red). No CD20-positive B lymphocytes in the vessel segment 2 cm proximal to the implanted stent (subject no. 291/96). (Magnification ×45, reduced by 65%.)

Inflammatory response. In addition to alpha-actin–positive SMCs up to nine months after stenting, increasing CD3-positive (Fig. 3A) and CD20-negative T lymphocytes (Fig. 3B) and CD68-positive cells of the monocyte–macrophage system are found. Later phases of stent incorporation show diffuse infiltration of CD3-positive and CD20-negative T lymphocytes in the neointima (Fig. 3, C and D). Directly adjacent to the alloplastic stent filaments are some multinucleated giant cells. CD68-positive macrophages accumulate in the intramural bleeding zones near intimal dissections. CD3-positive T lymphocyte aggregation is limited to the neointimal zone only. Proximal and distal artery segments show no infiltration by lymphocytes (Fig. 3, E and F). Immunohistochemical staining (CD20) revealed no B lymphocytes in the neointima. In the direct neighborhood of the alloplastic stent filaments only rare alpha-actin–positive SMCs were detected. The alloplastic stent filaments were separated from cellular components by a thin, acellular fiber-tissue zone (Fig. 2B). No foreign body granuloma was detected in the study group.

Neoendothelium. PHASE I: ENDOTHELIAL DENUDATION. Positive cells of endothelial origin tested by factor VIII are not found on the luminal surface of the neointima in the early phase of stent integration.

PHASE II: REENDOTHELIALIZATION. Even six weeks after stenting, the luminal border is not covered by mature factor VIII–positive endothelium (Fig. 2C). Alpha-actin–positive SMCs are reaching up to the luminal surface of the neointima, constituting the borderline between the neointima and lumen in this reparative phase.

PHASE III: NEOENDOTHELIUM. Complete coverage of the neointima by factor VIII–positive endothelial cells (neoendothelialization) is first found 96 days after stenting (Fig. 2D).

DISCUSSION

The major in vitro and in vivo studies available demonstrate a response to injury of the coronary vessel wall after conventional balloon angioplasty (percutaneous transluminal coronary angioplasty). During this neointimal repair initially proliferation and migration of SMCs, as well as expression of intracellular matrix and a later phase of inflammatory response with cell invasions like macrophages and lymphocytes, can be demonstrated (16,17).

The inflammatory response after implantation of coronary stents has been shown previously (15,18,19). In addition, it has been shown that especially the area around the stent struts shows an increased number of proliferating SMCs as well as infiltration of macrophages and leukocytes (18,20). During the six months after stent implantation a definite tissue response might lead to a reduction of the lumen size in certain areas due to increased intimal proliferation. Finally the stents are integrated in a proliferating tissue called "neointima," leading to incorporation and neutralization of the alloplastic stent material. In the first six months after stenting, a hyperproliferative tissue response may occur, producing continuous narrowing of the lumen cross-sectional area and diminishing the early luminal gain after interventional therapy. In clinical angiographic and IVUS studies, restenosis rates (<50% of the initial reference diameter) of 32% are documented (5). In 10% to 15% of the patients target lesion revascularization procedures are needed to treat in-stent restenosis (21). Proliferating endothelial cells do not contribute to neointima generation, as documented in pathologic-anatomic case reports on human atherectomy material (18,22).

Neointima. In accordance with the description of 11 human probes after stenting by Komatsu et al. (20) and in congruence with animal studies (12,13), the main component of the neointima is alpha-actin–positive SMCs.

Our findings propose two time phases with different morphologic stages of neointima generation. The first reparative phase is characterized by coverage of the implantation zone by a thin, membranous thrombus. Over the time course of incorporation this thrombus is infiltrated by SMCs secreting extracellular matrix.

In the second proliferative phase increasing numbers of SMCs and matrix lead to a volume gain of neointima. In this second phase the neointimal tissue shows a three-layered structure.

In none of the studied cases were the alpha-actin–positive SMCs found directly neighboring stent struts. In every phase of incorporation the alloplastic material is completely surrounded by an up to 40-μm-thick layer of acellular matrix. This may be caused by cytotoxicity of the implanted alloplastic stents. All studied stents consisted of chromium-nickel-ferrum (L-316) stainless steel (23).

In addition to SMCs, T lymphocytes and CD68-positive cells infiltrate the neointima. This cellular immigration was already described after experimental stenting in an animal model (24,25). Accumulation of these reactive inflammatory cells is limited to the stent zone and cannot be found in proximal and distal vessel segments. Directly adjacent to the alloplastic stent struts are inflammatory cells, usually aggregated, and foreign body macrophages can be detected, alluding to a possible immunologic cellular response to the chromium-nickel alloy.

Neoendothelium. The response of the endothelium to coronary stenting can be divided into three phases, as also seen in animal studies. Up to 16 days after stenting complete destruction of the endothelial cell layers, as an effect to the implantation trauma after coronary stenting, can be found. This severe endothelial alteration, as also seen after balloon injury (26) and atherectomy (27,28), initiates the formation of a thin, membranous thrombus covering the vascular and stent surface. This thrombus functions as the endoluminal layer of the vessel wall in the first weeks after stenting.

Up to 12 weeks after stent insertion only alpha-actin–positive SMCs can be detected on the surface of the generated neointima. Because of the endothelial denudation in the initial phase of stent implantation, alpha-actin–positive SMCs separate the vessel lumen and vessel wall. Mature endothelial cells act not only as a physiologic barrier against insudation into the vessel wall, but also as modulators of vascular tonus (29) and regulators of SMC proliferation (30). In this way, missing mature endothelium in the early incorporation phase and late reendothelialization may act as a cofactor in the process of exaggerative SMC proliferation.

Twenty-one days after balloon dilation of carotid arteries of swine, reendothelialization was observed (31). Complete endothelialization after experimental stenting in dogs was found after eight weeks (32). In our study on human coronary probes, mature endothelium (factor VIII–positive cells of endothelial origin) completely covering the neointima was first documented 96 days after stenting.

Although different types of stents were analyzed in our study, we found a uniform incorporation pattern in histomorphologic and immunohistochemical analysis. After implantation of coil stents and tubular stents, identical cellular and matrix compositions were found. Considering all implanted stents consisting of surgical L-316 stainless steel, the documented inflammatory response may be a response

to the implanted chromium-nickel alloy. Statistical analysis of stent–neointima volume with regard to the implanted stent design is not possible owing to the low case numbers in this study. The tissue response after stenting of venous aortocoronary bypasses does not differ from the incorporation process after stent implantation in coronary artery stenoses (11).

We were not able to definitely identify the pathogenesis of hyperproliferative neointima generation after stent insertion in our pathologic-anatomic study. The significant augmentation of inflammatory cells, especially of T lymphocytes, may preserve the stimulus to the hyperproliferative SMC response caused by the implantation trauma. Whether the inflammatory response is only *initiated* by the trauma of implantation—and perpetuated by the cytotoxicity of the chromium-nickel material—must be studied in further experiments. Accumulation of CD68-positive cells (macrophages) is due to intramural neointimal and medial hematoma. Spontaneous dissections can be observed even months after the stenting procedure. As observed in cellular cultures, activated macrophages produce platelet-derived growth factor, which is one of the strongest mitogenic stimuli on SMCs. Furthermore, the long period before complete reendothelialization may be a cofactor causing neointimal hyperplasia by SMC proliferation (33).

Reprint requests and correspondence: Dr. Peter H. Grewe, Department of Cardiology and Angiology, University Hospital "Bergmannsheil" Bochum, Bürkle-de-la-Camp-Platz 1, 44789 Bochum, Germany. E-mail: PeterGrewe@AOL.com.

REFERENCES

1. Colombo A, Hall P, Nakamura S, et al. Intracoronary stenting without anticoagulation accomplished with intravascular ultrasound guidance. Circulation 1995;91:1676–88.
2. Schömig A, Neumann FJ, Kastrati A, et al. Randomized comparison of antiplatelet and anticoagulant therapy after the placement of coronary-artery stents. N Engl J Med 1996;334:1084–9.
3. The EPIC Investigators. Use of a monoclonal antibody directed against the platelet glycoprotein IIb/IIIa receptor in high-risk coronary angioplasty. N Engl J Med 1994;330:956–61.
4. Moussa I, Oetgen M, Roubin G, et al. Effectiveness of clopidogrel and aspirin versus ticlopidine and aspirin in preventing stent thrombosis after coronary stent implantation. Circulation 1999;99:2364–6.
5. Serruys PW, de Jaegere P, Kiemeneij F, et al., for the BENESTENT Study Group. A comparison of balloon-expandable-stent implantation with balloon angioplasty in patients with coronary artery disease. N Engl J Med 1994;331:489–95.
6. Savage MP, Fischman DL, Schatz RA, et al., for the Palmaz-Schatz Stent Study Group. Long-term angiographic and clinical outcome after implantation of a balloon-expandable stent in the native coronary circulation. J Am Coll Cardiol 1994;24:1207–12.
7. Painter JA, Mintz GS, Wong SC, et al. Serial intravascular ultrasound studies fail to show evidence of chronic Palmaz-Schatz recoil. Am J Cardiol 1995;75:398–400.
8. Keane D, Azar AJ, de Jaegere P, et al. Clinical and angiographic outcome of elective stent implantation in small coronary vessels: an analysis of the BENESTENT trial. Semin Interv Cardiol 1996;1:255–62.
9. Peters RJG, Kok WE, Di Mario C, et al. Prediction of restenosis after balloon angioplasty: results of the PICTURE (Post-Intra Coronary Treatment Ultrasound Result Evaluation)—a prospective multicenter intracoronary ultrasound imaging study. Circulation 1997;95:2254–61.
10. Hoffman R, Mintz GS, Dussaillant RG, et al. Patterns and mechanisms of in-stent restenosis: a serial intravascular ultrasound study. Circulation 1996;94:1247–54.
11. Kearney M, Pieczek A, Haley L, et al. Histopathology of in-stent restenosis in patients with peripheral artery disease. Circulation 1997; 95:1998–2002.
12. Schatz RA, Palmaz JC, Tio FO, et al. Balloon-expandable intracoronary stents in the adult dog. Circulation 1987;76:450–7.
13. Hanke H, Kamenz J, Hassenstein S, et al. Prolonged proliferative response of smooth muscle cells after experimental intravascular stenting. Eur Heart J 1995;16:785–93.
14. Farb A, Sangiorgi G, Carter AJ, et al. Pathology of acute and chronic coronary stenting in humans. Circulation 1999;99:44–52.
15. Schwartz RS, Murphy JG, Edwards WD, et al. Restenosis after balloon angioplasty: a practical proliferative model in porcine coronary arteries. Circulation 1990;82:2190–2200.
16. McLeod DC, Strauss BH, de Jong M, et al. Proliferation and extracellular matrix synthesis of smooth muscle cells cultured from human coronary arteriosclerotic and restenotic lesions. J Am Coll Cardiol 1994;23:59–65.
17. Nobuyoshi M, Kimura T, Ohishi H, et al. Restenosis after percutaneous transluminal coronary angioplasty: pathologic observations in 20 patients. J Am Coll Cardiol 1991;17:433–9.
18. Anderson PG, Bajaj RK, Baxley WA, Roubin GS. Vascular pathology of balloon-expandable coil stents in humans. J Am Coll Cardiol 1992;19:372–81.
19. Groves PH, Banning AP, Penny WJ, et al. Kinetics of smooth muscle cell proliferation and intimal thickening in a pig carotid model of balloon injury. Arteriosclerosis 1995;117:83–96.
20. Komatsu R, Ueda M, Naruko T, et al. Neointimal tissue response at sites of coronary stenting in humans: marcroscopic, histological, and immunohistochemical analyses. Circulation 1998;98:224–33.
21. Fischman DL, Leon MB, Baim DS, et al., for the Stent Restenosis Study Group. A randomized comparison of coronary-stent placement and balloon angioplasty in the treatment of coronary artery disease. N Engl J Med 1994;331:496–501.
22. Strauss BH, Umans VA, Sylenv RJ, et al. Directional atherectomy for treatment of restenosis within coronary stents: clinical, angiographic and histologic results. J Am Coll Cariol 1992;20:1465–73.
23. Grewe PH, Machraoui A, Deneke T, et al. Strukturanalyse von 16 verschiedenen Coronarstentsystemen Z Kardiol 1997;86:990–9.
24. Karas SP, Gravains MG, Satoian EC, et al. Coronary intimal proliferation after balloon injury and stenting in swine: an animal model of restenosis. J Am Coll Cardiol 1992;20:467–74.
25. Gonschior P, Gerheuser F, Lehr HA, et al. Ultrastructural characteristics of cellular reaction after experimentally induced lesions in the arterial vessel. Basic Res Cardiol 1995;90:160–6.
26. Reidy MA, Clowes AW, Schwartz SM. Endothelial regeneration. V. Inhibition of endothelial regrowth in arteries of rat and rabbit. Lab Invest 1983;49:569–75.
27. Gonschior P, Gerheuser F, Gonschior GM, et al. Experimental directional atherectomy injury in arterial vessels: impact of trauma depth on cellular response. Am Heart J 1995;129:1067–77.
28. Taylor AJ, Farb AA, Angello DA, et al. Proliferative activity in coronary atherectomy tissue: clinical, histopathologic, and immunohistochemical correlates. Chest 1995;108:815–20.
29. Furchgott RF, Zawadzki JV. The obligatory role of endothelial cells in the relaxation of arterial smooth muscle by acetylcholine. Nature 1980;288:373–6.
30. Ross R, Raines EW, Bowen-Pope DF. The biology of platelet-derived growth factor. Cell 1986;46:155–69.
31. Carter AJ, Laird JR, Farb A, et al. Morphologic characteristics of lesion formation and time course of smooth muscle cell proliferation in a porcine proliferative restenosis model. J Am Coll Cardiol 1994;24: 1398–405.
32. Palmaz JC, Sibbitt RR, Reuter SR, et al. Expandable intraluminal graft: a preliminary study (work in progress). Radiology 1985;156: 73–7.
33. van Beusekom HM, Whelan DM, Hofma SH, et al. Long-term endothelial dysfunction is more pronounced after stenting than after balloon angioplasty in porcine coronary arteries. J Am Coll Cardiol 1998;32:1109–17.